31st Annual International Conference of the IEEE EMBS
Minneapolis, Minnesota, USA, September 2-6, 2009

Skin-electrode circuit model for use in optimizing energy transfer in volume conduction systems

Steven A. Hackworth, Mingui Sun, and Robert J. Sclabassi

Abstract—**The X-Δ model for through-skin volume conduction systems is introduced and analyzed. This new model has advantages over our previous X model in that it explicitly represents current pathways in the skin. A vector network analyzer is used to take measurements on pig skin to obtain data for use in finding the model's impedance parameters. An optimization method for obtaining this more complex model's parameters is described. Results show the model to accurately represent the impedance behavior of the skin system with error of generally less than one percent. Uses for the model include optimizing energy transfer across the skin in a volume conduction system with appropriate current exposure constraints, and exploring non-linear behavior of the electrode-skin system at moderate voltages (below ten) and frequencies (kilohertz to megahertz).**

Keywords— **skin model, volume conduction, energy transfer, optimization, implantable devices**

I. Introduction

IMPLANTABLE devices hold great potential for treating a number of diseases and conditions. However, many devices remain simply laboratory research tools and never reach clinical application due to practical difficulties with powering and communication. Our group has developed volume conduction as a platform technology to solve these problems for a variety of implantable device applications, such as drug delivery, stimulation, and physiological monitoring [1,2]. Volume conduction has unique advantages of being a low power, secure, and relatively easily implemented technology. To completely engineer any such system, an accurate model must be used. Previous skin models have been explored thoroughly [3], though most of these are mainly applicable in the area of tissue suspensions and low frequency, low voltage situations. This paper details a new model, the X-Δ model, which can be used in the design and optimization of implantable volume conduction systems, which typically use higher frequencies on the order of tens to hundreds of kilohertz and voltages on the level of one to ten volts.

Manuscript received April 7, 2009. This work was supported in part by U.S. Army Medical Research and Material Command contract No. W81XWH-050C-0047 to Computational Diagnostics, Inc. Pittsburgh, PA.

The authors are with the Laboratory for Computational Neuroscience, Departments of Neurological Surgery, Electrical & Computer Engineering, and Bioengineering, University of Pittsburgh, Pittsburgh, PA 15260, USA. (phone: 412-802-6481; e-mail: mrsun@neuronet.pitt.edu).

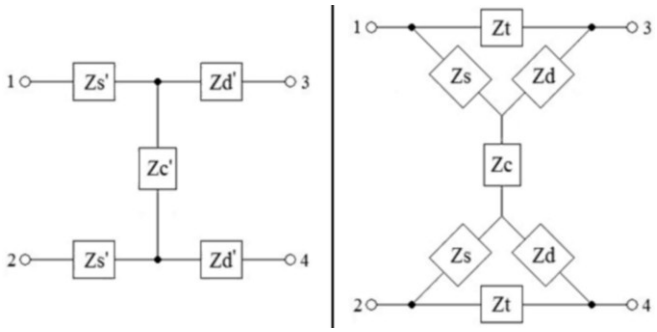

Fig. 1. Left: Symmetric X model from previous work. Right: Currently proposed X-Δ model for the developed volume conduction system. Terminals 1 and 2 connect to the external circuitry and terminals 3 and 4 connect to an internally implanted device.

II. Description of the Model

The proposed X-Δ model is shown in the right panel of Fig. 1. It is an extension of the simpler X model (left panel) from previous work, described in [2, 4]. In both models, terminals 1 and 2 represent connections to the external circuit outside of the skin, and terminals 3 and 4 represent connections to the device inside the body. The impedances along each branch represent current pathways through the skin. Inherent in the vertical symmetry of the models is the assumption that the skin is uniform in the small area required for the electrode connections, and that said connections are relatively similar on the same side of the skin. Although the X-Δ model is technically equivalent to the X model (see Table II), its importance lies in its more accurate representation of the pathways actually taken by current injected into the skin using the developed volume conduction system [1]. To clearly illustrate this behavior, a finite element analysis (FEA) model was used to simulate electrical behavior within the volume conduction system. Fig. 2 shows the model layout and resulting relative current densities (arrows) after simulation. The four smaller rectangular volumes, representing electrodes, have the same conductivity as copper (5.96×10^7 S/m), the leftmost large rectangle, representing the skin, has the same conductivity as skin tissue at approximately 100 KHz (0.07 S/m) [5], and the rightmost large rectangle simulates an attached device load of ~50 Ω. Stimuli of positive and negative five volts were applied to the leftmost "external" electrodes. Comparing Fig. 1 and Fig. 2, it can be seen that the X-Δ model explicitly represents the current pathways denoted by the arrows, whereas the X model is unable to do so. This makes the X-Δ model more valuable when imposing current exposure constraints during optimization of energy transfer in the system.

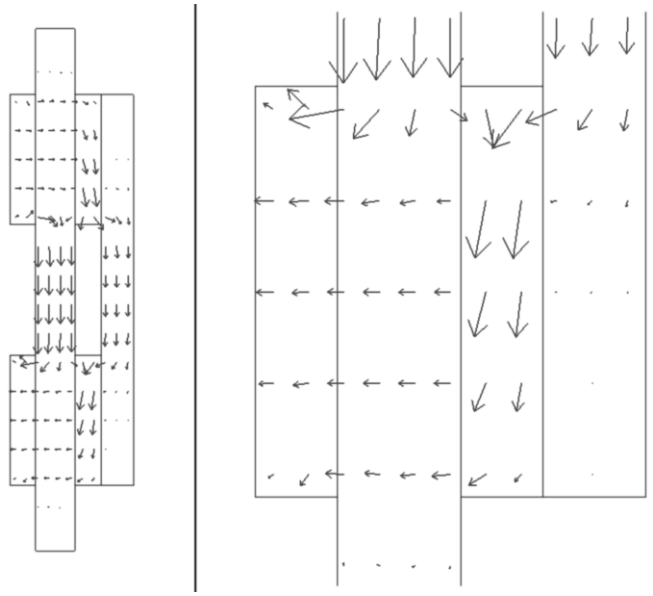

Fig. 2. Left: FEA model of the skin-electrode system with ±5-volt stimulus on the "external" (left) electrodes and a passive load on the "internal" (right) side. Arrows represent current density magnitude and direction. Right: Zoomed in view of the bottom part of the model, clearly showing the distribution of current between electrodes and the presence of a coupling current separate from the vertical cross current through the skin (*Zt* vs. *Zc*).

III. Experimental Procedures

To calculate values for the model parameters, impedance measurements across each pair of terminals (port) are needed. This section describes the methods used for obtaining said measurements.

A. Pig Skin Preparation and Setup

Pig skin was chosen due to its similarity to human skin tissue [6,7] and ease of acquisition. Six pieces of skin were harvested from the flanks of a pig, ranging in thickness from 4.5 mm to 7 mm. Hair was shaved off and the skin was slightly abraded on the external surface. Gold-plated semi-circular copper electrodes with surface areas of roughly 5 cm^2 were used to interface with the skin, forming four terminals (denoted by circles in Fig. 1). NuPrep™ conductive gel was applied to the external skin-electrode interface and a thin film of saline solution was used to keep the internal side of the skin moist. All measurements were taken within two hours of sacrifice in an attempt to keep electrical property changes small. It has been noted that tissue resistivity remains relatively constant within an hour after death, and even longer for certain tissues [8].

B. Vector Network Analyzer Measurements

After calibration, a vector network analyzer (VNA), model 8753ES, was connected to each possible pair of skin terminals to measure the associated impedances. Connections from the 50 Ω connector cable were kept as short as possible (~5 cm). The S11 port on the VNA provided 10 dBm power output across the frequency range from 30 KHz to 1 MHz, the target range of our volume conduction system. Both real and imaginary components of the impedances were recorded.

IV. Finding Model Parameters

To find the actual impedance values of the model, one needs to transform impedance measurements into model parameters. Table I gives the expressions for each model's equivalent port impedance measured across any two terminals. By using any three independent measurements for the X-model, e.g. Z_{12}, Z_{13}, and Z_{34}, and solving simple linear algebraic matrix equations, its impedance values can be calculated directly. This holds true even if the model is not symmetric [4]. However, the X-Δ model's impedance parameters cannot be calculated so easily. Here, we use an optimization method to find the impedance values which minimize the error between the measured impedances and the X-Δ model's equivalent port impedances.

The objective function to be optimized is a weighted sum of four individual error functions. Each individual error function takes the form of (1), where E_{ij} is a measure of the error between a particular impedance measurement Z_{ij} and the model's equivalent impedance M_{ij}, per Table I. *i,j* are the terminal numbers of the port across which the impedance was measured.

$$E_{ij} = \left|Z_{ij} - M_{ij}\right|^2 = \mathrm{Re}\left\{Z_{ij} - M_{ij}\right\}^2 + \mathrm{Im}\left\{Z_{ij} - M_{ij}\right\}^2 \qquad (1)$$

The objective function F can thus be expressed as

$$F = w_1 E_{12} + w_2 E_{13} + w_3 E_{14} + w_4 E_{34}, \qquad (2)$$

where w_k is a weight for each error function. Since each error function contains both real and imaginary parts of four independent variables, the solution search takes place over an eight-dimensional space. For simplicity, we set all weights equal to 0.5. A conjugate gradient method is used to realize the optimization, assuming the solution space is relatively convex. Step size during each iteration is determined by a golden section search method and the conjugate gradient algorithm is restarted after every eight iterations,

TABLE I
Two-Terminal Impedance Equivalents for X and X-Δ Models

Two-terminal Impedance	X Model	X-Δ model
Z_{12}	$2Zs'+Zc'$	$\frac{(Zt'+Zd')(2Zs'+Zc')+Zs'Zc'}{Zt'+Zd'+Zs'}$
$Z_{13} = Z_{24}$	$Zd'+Zs'$	$\frac{Zt'(Zd'+Zs')}{Zt'+Zd'+Zs'}$
$Z_{14} = Z_{23}$	$Zd'+Zs'+Zc'$	$\frac{(Zt'+Zc')(Zd'+Zs')+Zt'Zc'+2Zd'Zs'}{Zt'+Zd'+Zs'}$
Z_{34}	$2Zd'+Zc'$	$\frac{(Zt'+Zs')(2Zd'+Zc')+Zd'Zc'}{Zt'+Zd'+Zs'}$

TABLE II
X MODEL PARAMETER EQUIVALENTS FOR THE X-Δ MODEL

X Model Parameter	Equivalent Expression in X-Δ Model Parameters
Zd'	$\frac{ZtZd}{Zt+Zd+Zs}$
Zs'	$\frac{ZtZs}{Zt+Zd+Zs}$
Zc'	$\frac{2ZdZs}{Zt+Zd+Zs}+Zc$

corresponding to the dimension of the solution space. The optimization is performed separately for each frequency.

Because no constraints are imposed on the possible solutions, we propose a method to check if the optimized parameters are feasible. As mentioned earlier, the X-Δ model is technically equivalent to the X model, through a simple delta-wye transform. Thus converting the X-Δ model's parameters to their equivalent X model parameters, via Table II, and comparing them with the X model parameters calculated directly via linear equations should confirm that the optimization indeed arrives at a valid solution. Of course, an infinite number of possible X-Δ model parameters exist for any particular set of X model parameters, but no nonsensible solutions were found in practice. Many local minima were found, but these solutions were mostly similar in values.

V. IMPEDANCE RESULTS AND ERROR ANALYSIS

A. X-Δ Model Parameters

From the optimization method, impedance values for the X-Δ model parameters were found. Fig. 3 shows typical impedance curves for each piece of skin (6 mm in the figure) across the range of frequencies measured. *Zs* logically has the largest magnitude and large capacitive component, representing the multiple shallower layers of more resistive skin. *Zt* also has a large capacitive component, but the smallest magnitude, due to the large coupling between internal and external electrodes. *Zc* is mostly resistive, due to the non-capacitive current paths across the length of the skin. Interestingly, *Zd* has a positive phase and monotonically increasing magnitude, which both deserve further attention.

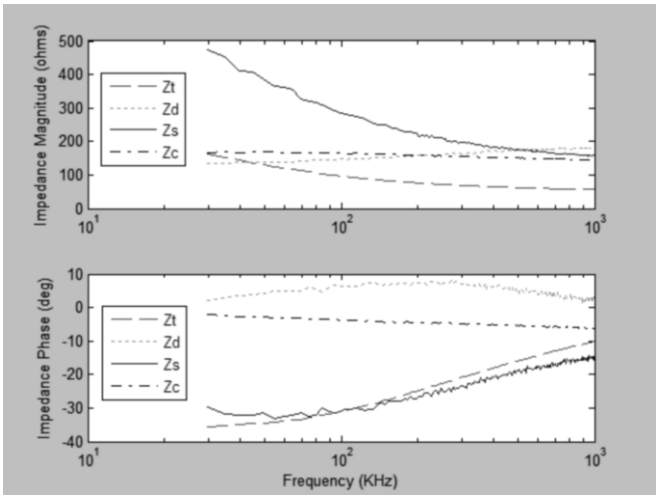

Fig. 3. X-Δ impedance parameters for 6 mm thick pig skin found using the conjugate gradient optimization method.

B. X-Δ Model Equivalent Port Impedance Error

To evaluate the accuracy of the X-Δ model, the errors between its equivalent port impedances (Table I) and the measured port impedances were calculated. Table III shows the average error across frequencies for each port and each piece of skin. Except for Z_{14}, error is consistently below 1%, with Z_{13} error even staying below 0.01%. This is likely due to its impedance being dominated by a single model parameter, *Zt*, which is mostly unaffected by impedances measured across other terminal pairs. Such small errors demonstrate that the X-Δ model accurately represents the electrical behavior of the system across the measured frequency range.

C. Equivalent X Model Parameter Error

As described in section III, the X-Δ model impedance results were converted into their X model equivalents to make sure the optimization method did not find a physically meaningless solution. Table IV shows the error between the directly calculated X model parameters (via linear equations) and the equivalent parameters calculated from the X-Δ model, per Table II. Clearly, the solution found by the optimization method coincides with the expected physically realizable solution, since all X model equivalent parameters are within 1% of the actual X model values.

TABLE III
ERROR BETWEEN MEASURED PORT IMPEDANCES AND THEIR CALCULATED X-Δ MODEL EQUIVALENTS

Skin Sample Thickness (±0.5 mm)	Error (%)			
	Z_{12}	Z_{13}	Z_{14}	Z_{34}
4.5 mm	0.854	0.005	1.690	0.880
4.5 mm	0.375	0.001	0.870	0.375
5.0 mm	0.391	0.003	0.765	0.383
6.0 mm	0.585	0.003	1.556	0.590
7.0 mm	0.727	0.006	6.337	0.692
7.0 mm	0.477	0.001	0.994	0.456

TABLE IV
ERROR BETWEEN X MODEL IMPEDANCE PARAMETERS AND THEIR CALCULATED X-Δ MODEL EQUIVALENTS

Skin Sample Thickness (±0.5 mm)	Error (%)		
	Zd'	*Zs'*	*Zc'*
4.5 mm	0.016	0.006	0.971
4.5 mm	0.002	0.002	0.458
5.0 mm	0.003	0.007	0.454
6.0 mm	0.007	0.003	0.693
7.0 mm	0.006	0.010	0.951
7.0 mm	0.001	0.001	0.636

VI. Discussion

From the minimal error results, it is clear that the X-Δ model describes the volume conduction system's behavior very well. Despite its being equivalent to the simpler X model, it has advantages in its explicit representation of the current pathways present in the system. This allows it to be used in energy transfer optimization processes with current limit constraints, as the current through any of the model's elements has a clear analog in the physical world. Such a process would focus on determining optimal values for the external and internal circuitry's input and output impedances so that power, current, or voltage transfer efficiencies could be maximized, depending on the application. Additionally, the model's parameters depend highly upon the electrode-skin geometry. Electrode separation, shape, and size all affect the impedance properties. Further investigation can reveal the dependence of each of the model's parameters upon such geometry variables, adding a further means of system optimization for any given size or shape constraint.

Beyond system optimization, the X-Δ model also provides insight into how certain parts of the skin behave when exposed to various stimuli. The unexpected positive phase of the *Zd* element is unseen in the X model's parameters, but may be an important indication as to the electrical behavior of the skin at such frequencies. Of course, the possibilities of measurement error (the VNA is sensitive to unmatched connections) or invalid model assumptions are additional options, but this matter deserves further attention before a conclusion can be made.

As far as the authors know, investigation into effects of voltages and frequencies on the order used in this volume conduction system is a relatively unexplored area. Most studies have focused on high voltage, pulsed stimuli (for surgical monitoring or electroporation), moderate voltage, low frequency stimuli (for iontophoresis), moderate voltage, high frequency stimuli (for RF energy transfer), or low voltage, low frequency stimuli (for experimental monitoring) [9-13]. As such, common models used in those studies, such as constant phase elements to describe frequency dispersion in the epidermis [13,14], are not applicable to the present area. Similarly, in [15], the limit current of linearity for electrode-electrolyte interfaces is shown to increase with increasing frequency, but data above 10 KHz is absent. Thus, in further refinement and use of this model, any assumptions concerning (non)linearity must be carefully considered (no such assumptions are made in this paper). The authors hope that future experiments focused on illuminating the skin system's behavior over our operating region and defining the limits of the X-Δ model will help establish volume conduction as an applicable technology for implantable devices.

Acknowledgment

S. A. Hackworth gratefully acknowledges the help and guidance of Professor Marlin H. Mickle and Leo Mats of the RFID Center of Excellence, Electrical & Computer Engineering, University of Pittsburgh, in addition to the use of their measurement instruments and many valuable suggestions.

References

[1] S.A. Hackworth, M. Sun, and R.J. Sclabassi, "A prototype volume conduction platform for implantable devices," in *Conf. Proc. 2007 IEEE NEBC*, pp. 124-125.

[2] M. Sun, S.A. Hackworth, Z. Tang, G. Gilbert, S. Cardin, and R.J. Sclabassi, "How to Pass Information and Deliver Energy to a Network of Implantable Devices within the Human Body," in *Conf. Proc. 2007 IEEE EMBS*, pp. 5286-5289.

[3] A.F. Coston and J.K-J. Li, "Transdermal drug delivery: a comparative analysis of skin impedance models and parameters," in *Conf. Proc. 2003 IEEE EMBS*, pp. 2982-2985.

[4] Z. Tang, R. J. Sclabassi, C. Sun, S. A. Hackworth, J. Zhao, X. T. Cui, *et al.*, "Transcutaneous battery recharging by volume conduction and its circuit modeling," in *Conf. Proc. 2006 IEEE EMBS*, pp. 644-647.

[5] S. Gabriel, R.W. Lau, and C. Gabriel, "The dielectric properties of biological tissues: II. Measurements in the frequency range 10 Hz to 20 GHz," *Phys. Med. Biol.*, vol 41, pp. 2251-2269, 1996.

[6] B. Godin and E. Touitou, "Transdermal skin delivery: Predictions for humans from *in vivo*, *ex vivo* and animal models," *Adv. Drug Deliv. Rev.*, vol. 59, pp. 1152-1161, 2007.

[7] U. Jacobi, M. Kaiser, R. Toll, S. Mangelsdorf, H. Audring, N. Otberg, *et al.*, "Porcine ear skin: an *in vitro* model for human skin," *Skin Research Tech.*, vol. 13, pp. 19-24, 2007.

[8] G.W. Crile, H.R. Hosmer, and A.F. Rowland, "The electrical conductivity of animal tissues under normal and pathological conditions," *Amer. J. Physiol.*, vol. 60, pp. 59-106, 1922.

[9] A. Jadoul, J. Bouwstra, and V. Préat, "Effects of iontophoresis and electroporation on the stratum corneum, Review of the biophysical studies," *Adv. Drug Deliv. Rev.*, vol. 35, pp. 89-105, 1999.

[10] J.E. Riviere and M.C. Heit, "Electrically-Assisted Transdermal Drug Delivery," *Pharma. Research*, vol. 14(6), pp. 687-697, 1997.

[11] S.K.S. Gupta, S. Lalwani, Y. Prakash, E. Elsharawy, and L. Schwiebert, "Towards a Propagation Model for Wireless Biomedical Applications," in *Conf. Proc. 2003 IEEE ICC*, pp. 1993-1997.

[12] A.J. Johansson, "Wireless Communication with Medical Implants: Antennas and Propagation," Ph.D. Dissertation, Lund University, Lund, Sweden, 2004.

[13] S. Grimnes and Ø.G. Martinsen, "Bioimpedance & Bioelectricity Basics," Academic Press, San Diego, CA, 2000.

[14] C-S. Poon and T.T.C. Choy, "Frequency dispersions of human skin dielectrics," *Biophys. J.*, vol. 34, pp. 135-147, Apr 1981.

[15] E.T. McAdams and J. Jossinet, "A Physical Interpretation of Schwan's Limit Current of Linearity," *Ann. Biomed. Engr.*, vol. 20, pp. 307-319, 1992.